Structure and electrical properties of a one-dimensional polymeric silver thiosaccharinate complex with argentophilic interactions

Mariana Dennehy, Pilar Amo-Ochoa, Eleonora Freire, Sebastián Suárez, Emilia Halac and Ricardo Baggio

IUCr Journals
CRYSTALLOGRAPHY JOURNALS ONLINE

Structure and electrical properties of a one-dimensional polymeric silver thiosaccharinate complex with argentophilic interactions

Mariana Dennehy,[a]* Pilar Amo-Ochoa,[b] Eleonora Freire,[c,d]‡ Sebastián Suárez,[e]‡ Emilia Halac[c,d] and Ricardo Baggio[c]*

[a]Departamento de Química (INQUISUR), Universidad Nacional del Sur, Bahía Blanca, Argentina, [b]Departamento de Química Inorgánica, Facultad de Ciencias, Universidad Autónoma de Madrid, Madrid, Spain, [c]Gerencia de Investigación y Aplicaciones, Centro Atómico Constituyentes, Comisión Nacional de Energía Atómica, Buenos Aires, Argentina, [d]Escuela de Ciencia y Tecnología, Universidad Nacional General San Martín, Buenos Aires, Argentina, and [e]Departamento de Química Inorgánica, Analítica y Química, Física/INQUIMAE–CONICET, Facultad de Ciencias Exactas y Naturales, Universidad de Buenos Aires, Buenos Aires, Argentina. *Correspondence e-mail: mdennehy@uns.edu.ar, baggio@tandar.cnea.gov.ar

Among the potential applications of coordination polymers, electrical conductivity ranks high in technological interest. We report the synthesis, crystal structure and spectroscopic analysis of an Ag^I–thiosaccharinate one-dimensional coordination polymer {systematic name: *catena*-poly[[[aquatetrakis(μ_3-1,1-dioxo-1,2-benzisothiazole-3-thiolato-$\kappa^3 N$:S^3:S^3)tetrasilver(I)]-μ_2-4,4′-(propane-1,3-diyl)dipyridine-$\kappa^2 N$:$N′$] dimethyl sulfoxide hemisolvate]}, {[$Ag_4(C_7H_4NO_2S_2)_4$-$(C_{13}H_{14}N_2)(H_2O)$]·$0.5C_2H_6OS$}$_n$, with the 4,4′-(propane-1,3-diyl)dipyridine ligand acting as a spacer. A relevant feature of the structure is the presence of an unusually short Ag$\cdots$Ag distance of 2.8306 (9) Å, well within the range of argentophilic interactions, confirmed experimentally as such by a Raman study on the low-frequency spectrum, and corroborated theoretically by an Atoms in Molecules (AIM) analysis of the calculated electron density. Electrical conductivity measurements show that this complex can act as a semiconductor with moderate conductivity.

1. Introduction

The synthesis of coordination compounds with Ag^I metal centres results in a large panoply of different structural motifs, even when using similar starting coligands, due to the extreme coordination versatility of the Ag^I cation. In the case of silver thiosaccharinates, this characteristic has been widely tested (Burrow *et al.*, 2016).

In addition, coordination polymers are currently a trending topic due to the potential applications of their varied properties, among which electrical conductivity (EC) ranks high in technological interest (Givaja *et al.*, 2012).

In this work, we present the synthesis, structural characterization and electrical conductivity (EC) measurements of a new coordination polymer, denoted {[$Ag_4(tsac)_4(tmdp)$-(H_2O)]·$0.5DMSO$}$_n$, (I), where tsac is the thiosaccharinate anion, tmdp is 4,4′-(propane-1,3-diyl)dipyridine and DMSO is dimethyl sulfoxide.

In addition, the EC of (I) is compared with those of some related polymeric silver thiosaccharinates, *viz.* [$Ag_2(tsac)_2$-$(4,4′$-bipyridine)$_{1.5}$]$_n$, (II) (Dennehy *et al.*, 2016), and [Ag-$(tsac)(4$-$MeOpy)$]$_n$ (4-MeOPy is 4 methoxypyridine), (III) (Dennehy *et al.*, 2010), with the aim of explaining eventual EC differences in terms of their structural variations.
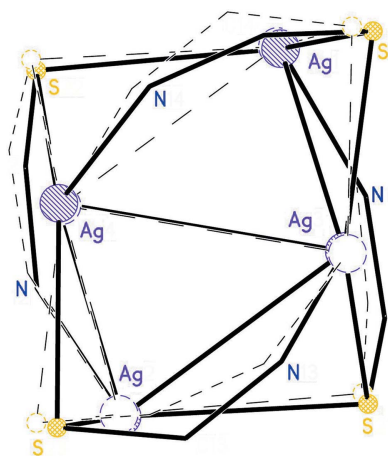
2. Experimental

2.1. Synthesis and crystallization

Compound (I) was synthesized by adding Htsac (12 mg, 0.06 mmol), $AgNO_3$ (10 mg, 0.06 mmol) and tmdp (24 mg, 0.12 mmol) (1:1:2 molar ratio, all solids) to dimethyl sulfoxide (2 ml). This resulted in a clear yellow solution into which CH_2Cl_2 (2 ml) was diffused slowly. Crystals suitable for structural study by X-ray diffraction had appeared after 10 d.

Scheme 1
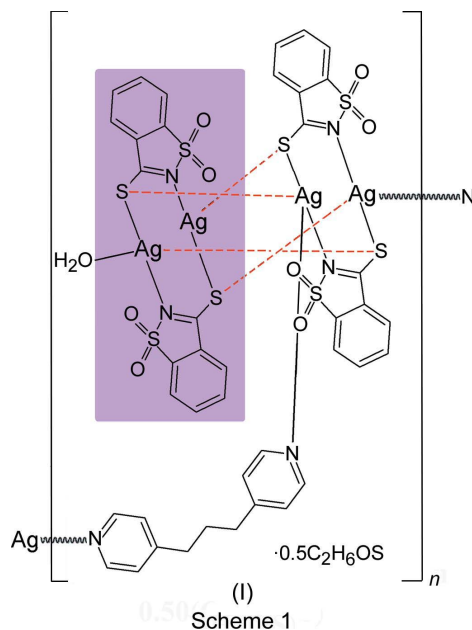
Analytical composition calculated for $C_{42}H_{35}Ag_4N_6O_{9.5}S_{8.5}$: C 34.09, H 2.38, N 5.67%; found: C 33.93, H 1.89, N 5.21%. FT–IR (ν, cm^{-1}): 3444 (vw), 1609 (m), 1462 (s), 1417 (m), 1321 (m), 1228 (m), 1168 (m), 1122 (w), 1001 (m), 796 (w), 768 (w), 626 (w), 587 (m), 555 (m), 534 (m), 430 (m).

Scheme 2
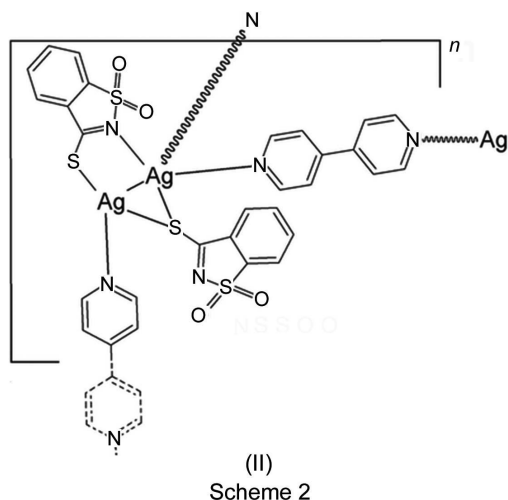
2.2. Refinement

Crystal data, data collection and structure refinement details for (I) are summarized in Table 1. Some metric and displacement-parameter restraints were used to refine the disordered DMSO solvent, and thus facilitate convergence. The occupation factor of the two disordered moieties

Table 1
Experimental details.

Crystal data	
Chemical formula	$[Ag_4(C_7H_4NO_2S_2)_4(C_{13}H_{14}N_2)(H_2O)] \cdot 0.5C_2H_6OS$
M_r	1479.75
Crystal system, space group	Triclinic, $P\bar{1}$
Temperature (K)	290
a, b, c (Å)	13.7710 (4), 13.9822 (4), 14.7181 (5)
α, β, γ (°)	81.074 (3), 79.523 (3), 73.152 (3)
V (Å^3)	2651.23 (15)
Z	2
Radiation type	Mo $K\alpha$
μ (mm^{-1})	1.85
Crystal size (mm)	$0.42 \times 0.30 \times 0.10$
Data collection	
Diffractometer	Rigaku OD Xcalibur Eos Gemini
Absorption correction	Multi-scan (CrysAlis PRO; Rigaku OD, 2015)
T_{min}, T_{max}	0.50, 0.85
No. of measured, independent and observed [$I > 2\sigma(I)$] reflections	26030, 11551, 7060
R_{int}	0.032
$(\sin \theta/\lambda)_{max}$ (Å^{-1})	0.682
Refinement	
$R[F^2 > 2\sigma(F^2)]$, $wR(F^2)$, S	0.056, 0.158, 1.03
No. of reflections	11551
No. of parameters	659
No. of restraints	62
H-atom treatment	H atoms treated by a mixture of independent and constrained refinement
$\Delta\rho_{max}$, $\Delta\rho_{min}$ (e Å^{-3})	1.17, −0.85

Computer programs: CrysAlis PRO (Rigaku OD, 2015), SHELXS97 (Sheldrick, 2008), XP in SHELXTL (Sheldrick, 2008), SHELXL2014 (Sheldrick, 2015) and PLATON (Spek, 2009).

wouldnot behave steadily in an independent refinement, so they were forced to add up to 0.50, roughly the oscillation mean value, after which refinement went smoothly. H atoms,

Scheme 3
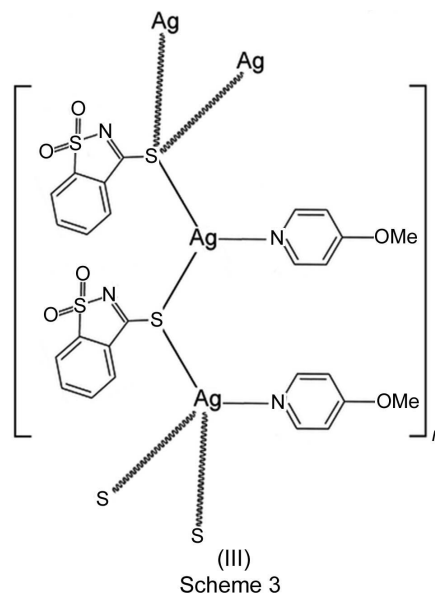
except those of the water ligand and the disordered DMSO solvent molecule, were found in a difference map. Those attached to C atoms were finally idealized and refined as

riding, with aromatic C—H = 0.93 Å and $U_{iso}(H) = 1.2U_{eq}(C)$, methylene C—H = 0.97 Å and $U_{iso}(H) = 1.2U_{eq}(C)$, and methyl C—H = 0.96 Å and $U_{iso}(H) = 1.5U_{eq}(C)$. The H atoms of the water molecule were assigned where the closest potential hydrogen-bonding acceptors were located and refined with idealized geometry afterwards, with $U_{iso}(H) = 1.5U_{eq}(O)$. The propylene C—C distances were subject to a similarity restraint.

Although there are about 2500 missing reflections above $\sin(\theta)/\lambda = 0.60$, we wanted to include as much high-angle data as possible. A trial refinement was made at a maximum 2θ value of 52°, to investigate if any introduced bias could be detected. Analysis of the results obtained in both refinements showed no perceivable differences regarding the quality of the final parameters (the maximum difference was found for a C—C bond length, of the order of 1/1500, with an s.u. value of 6/1500). But, in addition, we found that standard validation procedures (*checkCIF*) treated similar conflicting situations differently (in our case, a Hirshfeld difference with s.u. $\simeq$ 0.12), which in the refinement with the smaller data set would be ranked as a 'B alert', but as a much lighter 'G alert' with the whole data set. This seems to stress the benefit of using as much data as possible (irrespective of its distribution in reciprocal space), as long as uninformative noise is avoided.

2.3. Spectroscopic analysis and electrical conductivity measurements

IR spectra were obtained on an FT–IR–NIR Thermo Scientific Nicolet iS50 using KBr dispersions.

Raman spectra, in turn, were gathered with a LabRAM HR Horiba Jobin Yvon Raman system equipped with two monochromator gratings and a charge-coupled device detector. A 1800 g mm^{-1} grating and a 50 μm hole resulted in a spectral resolution of 1.5 cm^{-1}. The spectrograph is coupled to an imaging microscope with 10×, 50× and 100× magnifications. The He–Ne laser line at 632.8 nm is used as the excitation source. Each spectrum was averaged over eight scans with a collection time of 120 s for each scan. Raman spectra were acquired on powder samples at room temperature; measurements were carried out using a backscattering geometry, with 10× magnification.

Direct current (DC) electrical conductivity measurements were performed on different single crystals with carbon paint at 300 K and two contacts. The contacts were made with tungsten wires (25 μm diameter). The samples were measured at 300 K, applying an electrical current with voltages from +10 to −10 V. The electric current flowing through the sample as a consequence of the potential difference was recorded.

The samples were measured in a Quantum Design PPMS-9 connected to an external voltage source (Keithley model 2400 source-meter) and amperometer (Keithley model 6514 electrometer).

2.4. Atoms in Molecules (AIM) analysis

Density functional theory calculations were performed on a fragment of the polymeric complex containing the three putative Ag···Ag interactions. X-ray structures were used without geometry optimization. The Becke three-parameter exchange functional with a Lee–Yang–Parr correlation func-

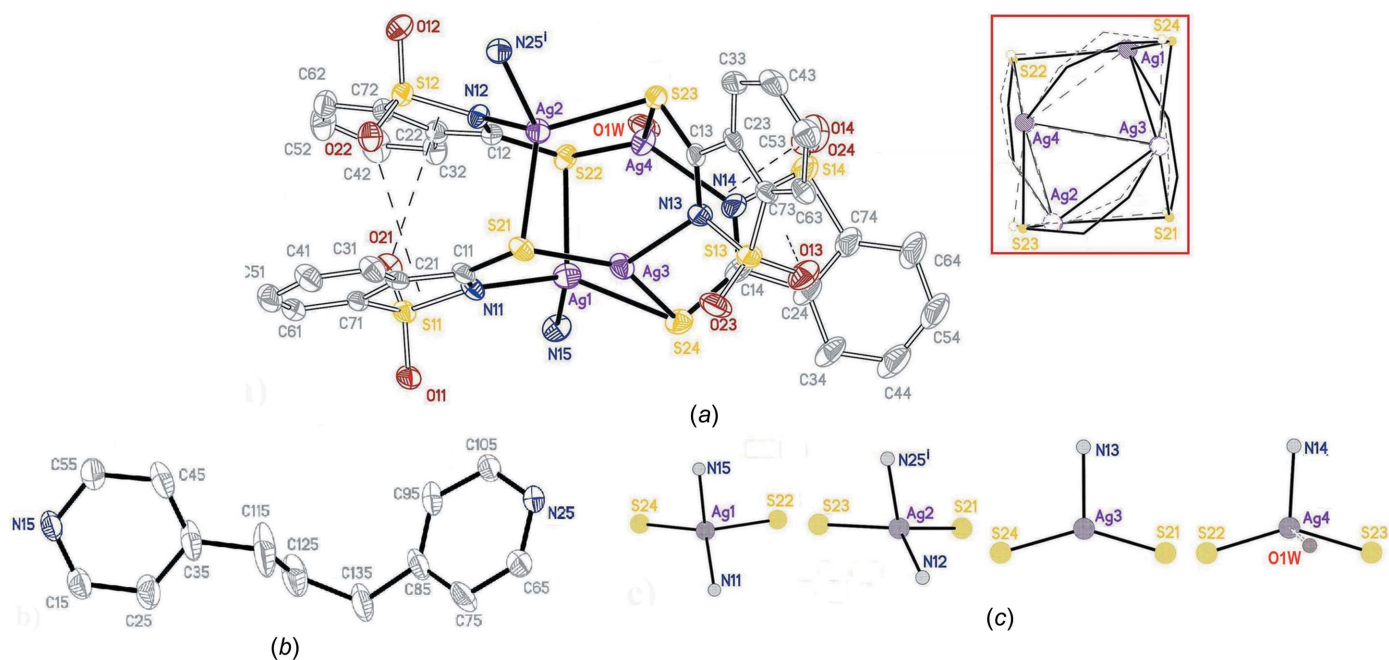**Figure 1**
(*a*) A view of the [Ag(tsac)]$_4$ conglomerate. Dashed lines denote interconglomerate S—O···π interactions. The inset shows a fitting of the conglomerate and its 'twofold' rotated image. (*b*) A view of the tmdp ligand, with displacement ellipsoids drawn at the 40% probability level. (*c*) The coordination polyhedra around the four independent Ag atoms.

Table 2
Selected bond lengths in (I) (Å).

Ag1—N15	2.307 (6)	Ag3—N13	2.317 (5)
Ag1—N11	2.422 (5)	Ag3—S21	2.416 (2)
Ag1—S22	2.607 (2)	Ag3—S24	2.472 (2)
Ag1—S24	2.647 (2)	Ag4—N14	2.354 (6)
Ag2—N12	2.320 (5)	Ag4—S22	2.461 (2)
Ag2—N25i	2.335 (6)	Ag4—S23	2.510 (2)
Ag2—S23	2.606 (2)	Ag4···O1W	2.612 (9)
Ag2—S21	2.615 (2)		
Ag1···Ag3	2.8307 (8)	Ag3···Ag4	3.0692 (9)
Ag2···Ag4	2.9180 (8)	Ag2···Ag3	3.3489 (8)

Symmetry code: (i) $x + 1$, y, $z - 1$.

Table 3
S=O···π bonds in (I).

O/perp is the perpendicular distance of the O atom to the plane, O···Cg/perp is the angle between the O···Cg vector and the plane normal, and S=O/perp is the angle between the S=O vector and the plane normal. $Cg1$ is the centroid of the S11/N11/C11/C21/C71 ring, $Cg2$ that of the S12/N12/C12/C22/C72 ring, $Cg3$ that of the S13/N13/C13/C23/C73 and $Cg4$ that of the S14/N14/C14/C24/C74 ring.

S=O···Cg	O···Cg (Å)	O/perp (Å)	O···Cg/perp (°)	S=O/perp (°)
S13=O13···$Cg4$	3.533 (8)	3.428	30.30	111.5 (3)
S14=O14···$Cg3$	3.718 (9)	3.440	13.41	115.5 (7)
S11=O21···$Cg2$	3.343 (6)	3.124	46.34	116.9 (3)
S12=O22···$Cg1$	3.388 (6)	3.244	41.68	116.6 (3)

tional (B3LYP) was used in the study (Becke, 1988, 1993; Serpe *et al.*, 2001). The Stuttgard–Dresden effective core potential along with the SDD valence basis set was used for Ag^I atoms (Fuentealba *et al.*, 1989; Cao & Dolg, 2002; Schwerdtfeger *et al.*, 1989), whereas all other atoms were treated with the 6-31G basis set (Ditchfield *et al.*, 1971; Rassolov *et al.*, 2001). The AIM analysis of the electron density was performed using the *Multiwfn* program (Lu & Chen, 2012).

3. Results and discussion

3.1. Structure analysis

The asymmetric unit of (I) consists of four Ag^I cations (Ag1 to Ag4), four anionic tsac ligands (tsac1 to tsac4) and one tmdp ligand. The formula is completed by one water molecule and half of a disordered DMSO solvent molecule. The tsac ligands are unexceptional, not departing from their expected geometry, and their most relevant role is the way in which they interact with the Ag^I cations, through a μ^3 coordination involving the exocyclic S atoms (bridging two metal centres)
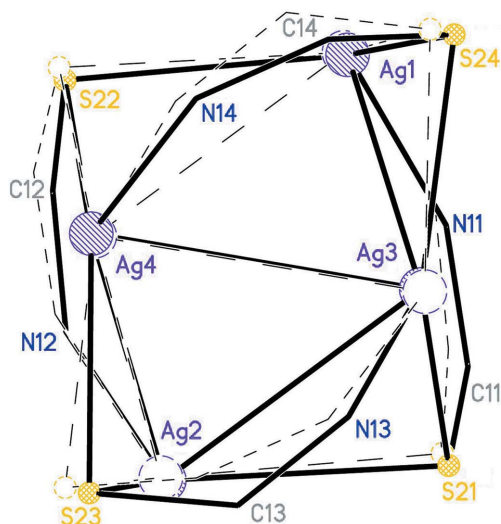

Figure 2
Least-squares fit of the Ag^I cations in the [AgSCN]$_4$ conglomerates of (I) (full lines) and XIHREM (dashed lines), disclosing the similarity in topology but differences in metrics.

and the endocyclic N atom, which define an [Ag(tsac)]$_4$ conglomerate (Fig. 1a). Table 2 presents selected coordination distances.

The fact that the four anions coordinate in a similar way is reflected in the IR spectrum, which shows only one absorption band for the anion. In the same spectrum (see Fig. S1 in the supporting information), the bands corresponding to the nitrogenated colligate can also be observed.

The resulting globular clusters are made up of two extremely similar [Ag(tsac)]$_2$ rings (highlighted in Scheme 1), further connected through four S—Ag bonds. In this sense, the cluster can be considered as a *dimer of dimers*. Even if this particular choice of rings is rather arbitrary, due to the two possible S—Ag bonds for each S atom, the one we appoint is sustained by a plausibility argument based on symmetry reasons, *viz.* the whole [Ag(tsac)]$_4$ group, as described herein, presents a kind of twofold pseudosymmetry, relating Ag1 with Ag2, and Ag3 with Ag4, as shown in the inset in Fig. 1. A search in the Cambridge Structural Database (CSD, Version 5.38 and updates; Groom *et al.*, 2016) disclosed that a very similar arrangement has been reported in Dennehy *et al.* (2007) (CSD refcode XIHREM), whose nucleus is also made up of two dimers linked by four S—Ag bonds, in a disposition analogous to that in (I). This similarity is confirmed in Fig. 2, which shows a least-squares fit of the Ag^I cations in both nuclei, making the identical topologies of both clusters apparent, while disclosing some significant metric differences, as discussed below.

The cohesion of the [Ag(tsac)]$_4$ group in (I) is further enhanced by four intramolecular S=O···π bonds, presented in Table 3 and shown in Fig. 1(a) as dashed lines. It is to be noted that all the exocyclic SO$_2$ groups, as well as all the five-membered rings are involved in these interactions.

The 4,4′-(propane-1,3-diyl)dipyridine (tmdp) molecule departs severely from coplanarity (Fig. 1b), with the planes of the terminal pyridine groups, denoted Py(N15) and Py(N25), defining dihedral angles with the C115–C135 central group of 113.2 (2) and 80.7 (2)°, respectively, and 34.5 (2)° with each other. The elongated ligand acts as a spacer between neighbouring [Ag(tsac)]$_4$ clusters, linking them (through atoms N15 and N25) to define chains parallel to [10$\bar{1}$] (Fig. 3). With the inclusion of these lateral tmdp ligands, Ag1 and Ag2 end up being four-coordinated in an AgN$_2$S$_2$ distorted tetrahedral
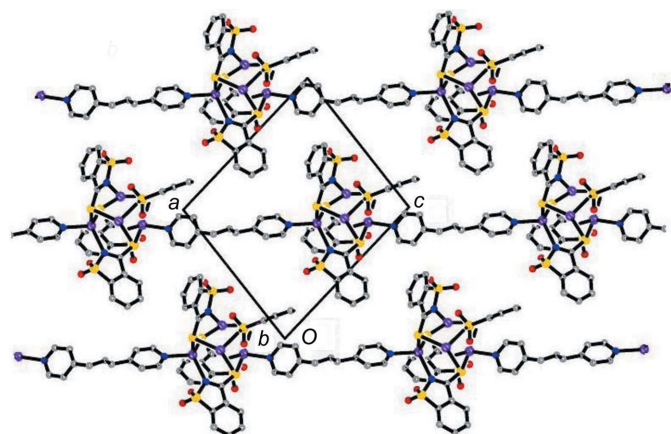
Figure 3
The parallel [10$\bar{1}$] chains, showing the 'knot' *versus* 'thread' disposition optimizing compactness.

Table 4
Hydrogen-bond geometry (Å, °).

$D-H\cdots A$	$D-H$	$H\cdots A$	$D\cdots A$	$D-H\cdots A$
O1W—H1WB⋯O14	0.95 (10)	2.59 (11)	3.425 (18)	147 (9)
O1W—H1WB⋯O24	0.95 (10)	2.59 (8)	3.072 (18)	112 (8)
O1W—H1WA⋯O1A^i	0.96 (9)	2.05 (18)	2.65 (2)	119 (12)
C125—H12B⋯O1W^i	0.97	2.53	3.369 (17)	144
C44—H44⋯O11^{ii}	0.93	2.52	3.260 (13)	137
C53—H53⋯S21^{iii}	0.93	2.86	3.572 (9)	134
C75—H75⋯O24^{iv}	0.93	2.41	3.284 (16)	158
C105—H105⋯S23^v	0.93	2.82	3.508 (9)	132

Symmetry codes: (i) $-x+1, -y+1, -z+1$; (ii) $-x+1, -y, -z+1$; (iii) $-x+2, -y, -z$; (iv) $x, y, z+1$; (v) $x-1, y, z+1$.

environment, while Ag3 and Ag4 are three-coordinated in a quasi-planar AgNS$_2$ environment, with the cations lying 0.06 (2) and 0.14 (2) Å from the least-squares plane defined by the ligands. In this sense, it is worth mentioning that water molecule O1W occupies a *pseudo-apical* site in the Ag4 polyhedron, at a quasi-coordination Ag⋯O distance of 2.612 (9) Å. Even if rather weak (AIM calculations suggest it to be comparable to a medium-strength O⋯H hydrogen bond), this type of Ag^I⋯OW interaction is not unusual; a search in the CSD found 130 cases of a comparable Ag$^I X_3$_OW ($X =$ S, N or O) polyhedra, with a mean Ag—OW coordination distance of 2.50 (15) Å and a 2.135–2.855 Å span, with the present case lying in the longest quartile.

The resulting coordination of each Ag^I cation can be seen qualitatively in Figs. 1(*a*) and 1(*c*), and quantitative details can be found in Table 2. The difference in coordination numbers is reflected in the Ag—S and Ag—N coordination distances, distinctly shorter in Ag3 and Ag4. The corresponding bond valence, as calculated by the program *Valence* (Brown, 2002), remains fairly constant, around the expected 1+ charge of the cation, *viz.* Ag1 = 0.943, Ag2 = 1.003, Ag3 = 1.075 and Ag4 = 1.036, with a total for all four cations of 4.057.

The one-dimensional substructure (the elemental unit building up the crystal structure) resembles a thin *wire* with evenly spaced bulky *protuberances* on it. In the packing process, the chains align parallel to each other but shift along the chain direction so as to have the protuberances facing the thin section in neighbouring chains (Fig. 3), and thus optimizing compactness. They are interconnected by weaker (interchain) noncovalent bonds, as well as a few more, mediated by the water ligands and DMSO solvent molecules (Table 4) interspersed between the chains. Regarding the latter DMSO molecule, it makes an S=O⋯O=S short contact to the S4—O24 group [O⋯O = 2.871 (2) Å].

3.2. Argentophilic interactions

A distinctive characteristic of silver thiosaccharinates is the fact that the different bridging modes displayed by the anion can lead to intricate crystal structures with short Ag⋯Ag distances. When these short contacts are interactive (and not the mere result of packing constraints), they are called *argentophilic interactions* (Kristiansson, 2001; Castiñeiras *et al.*, 2006; Schmidbaur & Schier, 2015).

These metallophilic contacts can be formed with or without the assistance of an anion or any other ligand bridging the metal cations. The proximity of the two Ag^I atoms may lead to strong d^{10}–d^{10} interactions and, as a rule of thumb, they are usually considered to be present for Ag⋯Ag distances shorter than 3.44 Å (twice the Ag^I van der Waals radius; Bondi, 1964). In the present structure of (I), there are four of these short Ag⋯Ag distances (Table 2).

A CSD survey of reported Ag⋯Ag distances in similar complexes disclosed that the 2.8307 (8) Å value in (I) is the second shortest found in silver thiosaccharinates, second only to the extremely effective centrosymmetric double bridge [μ_2-$\kappa^2 S$:S]$_2$ = (SAg$_2$S) present in XIHQUB (Dennehy *et al.*, 2008) and leading to a value of 2.789 Å. The remaining short distances found involve either (i) a combination of the μ_2-$\kappa^2 N$:S bite on one side plus a μ_2-$\kappa^2 S$:S bridge on the other, as in EPUMUZ (Dennehy *et al.*, 2016; d = 2.886 Å), or (ii) plainly the same head-to-tail [Ag(tsac)]$_2$ dimers found in (I). As a comparison, the values in the already discussed topologically similar XIHREM (2.952 and 3.000 Å), in spite of being within what is usually considered 'ligand-assisted' argentophilic interaction distances, are nonetheless significantly longer than the shortest distances found in (I), *viz.* 2.830 and 2.918 Å.

Argentophilic interactions are currently being studied both from experimental and theoretical points of view (*e.g.* Lamming *et al.*, 2017). Among the former studies, some reports in the literature show that the Ag⋯Ag stretching vibration may reveal the eventual presence (and strength) of a silver–silver interaction (Morishima *et al.*, 2014; Harvey, 1996). We have evaluated *argentophilic interactions* by means of Raman spectroscopy in a previous work (Dennehy *et al.*, 2016). The Raman spectrum of (I) (see Fig. S2 in the supporting information) also shows a weak stretching band at 78 cm^{-1} that could be assigned to the Ag⋯Ag vibrational mode and is consistent with the presence of an Ag⋯Ag metallophilic interaction in this complex. The Ag—S stretching modes are reflected in a band appearing at 249 cm^{-1} (Martina *et al.*, 2012). The bands at 366 cm^{-1} could be attributed to Ag—N stretching vibrations, while the bands at 116 and 153 cm^{-1} could be related to other Ag—N modes.

To complement those experimental studies, we have also approached the problem from a theoretical point of view, by way of an Atoms in Molecules (AIM) analysis (Bader, 1990), which for the detection of interatomic interactions analyses the values and shape of the calculated electron-density curve [$\rho(r)$], its gradient [$\nabla(r)$] and its Laplacian [$\nabla^2\rho(r)$]. (Further
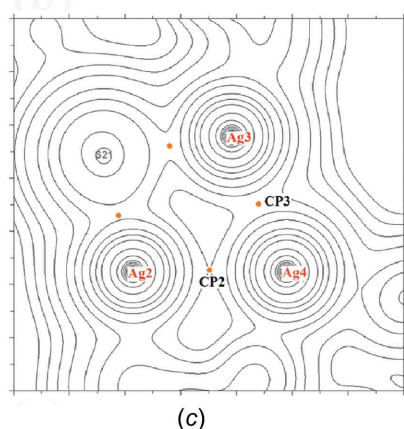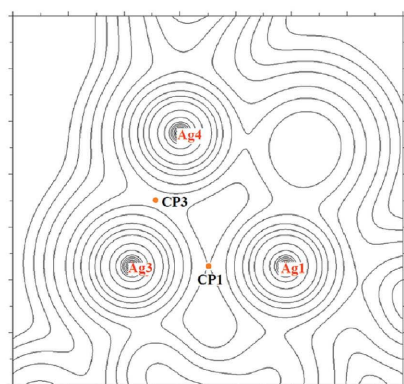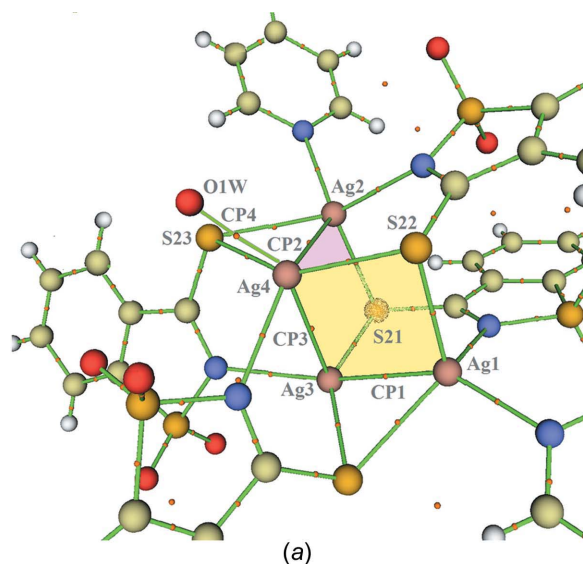

(a)

(b)

(c)

Figure 4
(a) Selected BCPs (orange balls) in (I). (b) Contour lines of the charge density in the Ag1–Ag3–Ag4 plane [highlighted in yellow in part (a)]. (c) Contour lines of the charge density in the Ag2–Ag3–Ag4 plane [highlighted in pink in part (a)]. Note the lack of BCPs in the Ag2–Ag3 and Ag1–Ag4 intermetallic zones.

Table 5
Comparison of the relative strengths of argentophilic interactions in (I) with those of selected covalent and noncovalent interactions.

Cg1 is the centroid of the S11/N11/C11/C21/C71 ring, Cg2 that of the S12/N12/C12/C22/C72 ring, Cg3 that of the S13/N13/C13/C23/C73 and Cg4 that of the S14/N14/C14/C24/C74 ring.

Interaction	#CP	Contact	Distance	$\rho(r)$ ($\times 100$)	$\nabla^2\rho(r)$ ($\times 10$)
Ag$\cdots$Ag	CP1	Ag1$\cdots$Ag3	2.8307 (8)	3.23	0.80
	CP3	Ag3$\cdots$Ag4	3.0692 (9)	1.99	0.51
	CP2	Ag4$\cdots$Ag2	2.9180 (8)	2.75	0.69
	CP4	Ag4$\cdots$O1W	2.612 (9)	2.66	0.85
O$\cdots\pi$		O13$\cdots$Cg4	3.533 (8)	0.37	0.14
		O14$\cdots$Cg3	3.718 (9)	0.36	0.15
		O21$\cdots$Cg2	3.343 (6)	0.68	0.25
		O22$\cdots$Cg1	3.388 (6)	0.53	0.19
S—Ag		S21—Ag3	2.416 (2)	7.21	1.90
		S21—Ag2	2.615 (2)	4.77	1.23
		S22—Ag1	2.607 (2)	4.85	1.25
		S22—Ag4	2.461 (2)	6.59	1.74
		S23—Ag2	2.606 (2)	4.90	1.25
		S23—Ag4	2.510 (2)	6.03	1.50
		S24—Ag1	2.647 (2)	4.63	1.17
		S24—Ag3	2.472 (2)	6.43	1.59

information on the method is given in the supporting information.)

The calculations made showed that there was a significant accumulation of electron density between Ag1$\cdots$Ag3, Ag2$\cdots$Ag4 and Ag3$\cdots$Ag4, confirmed by the presence of bond critical points (BCPs). In contrast, there was no BCP in the intermetallic region between Ag2$\cdots$Ag3, in accordance with the longer intermetallic distance (Fig. 4).

This kind of analysis has the advantage of allowing quantitative estimations of the interaction strengths, at least in relative terms, by comparison with other more familiar interactions in the structure.

This information is presented in Table 5, where in the two rightmost columns, the electron density and its Laplacian at the CP are shown.

From the values therein, it is clear that the strengths of the argentophilic interactions lie midway between those of coordination bonds and the weaker noncovalent interactions. However, the Ag1$\cdots$Ag3 contact is almost twice as strong as the remaining ones in Table 5, and comparable to the long Ag4—O1W coordination bond, thus highlighting its relevance.

3.3. Electrical conductivity

It has been stated that, in addition to the techniques mentioned above, as well as the short intermetallic distances, argentophilic interactions could be evidenced via some further physical properties of the complexes, such as electrical conductivity (EC) (Jansen, 1987; Su et al., 2000). In order to obtain clues about this eventual EC–argentophilicity relationship (the latter as qualitatively evaluated by the shortest Ag$\cdots$Ag distance in the structure) or on the way in which the crystal structure might influence this behaviour, we thought of comparing the EC values in (I) with those of related polymeric complexes presenting argentophilic contacts of varied strength

Table 6
Electric conductivity and argentophilic interactions in (I), (II) and (III).

Compound	EC (S cm^{-1})	Ag$\cdots$Ag (Å)	Bridging mode
(I)	2.5×10^{-8}	2.830	N—Ag
(II)	2.9×10^{-7}	2.886	N—Ag
(III)	9.5×10^{-3}	3.024	S—Ag

(= intermetallic distance), but with a rather similar [as in structure (II)] or a totally different [as in structure (III)] bridging connectivity (Scheme 2). With this idea in mind, we measured the corresponding ECs at $T = 300$ K in single crystals of all three compounds, wired with tungsten tips connected through a graphite tincture (details of the set-up can be seen in Fig. 5a) to end up with the curves shown in Fig. 5(b) and the values reported in Table 6. The ECs obtained indicate that all three polymers could be semiconductors with moderate conductivity. A comparative inspection suggests an extremely feeble (if any) correlation between the EC and the argentophilic interaction, but at the same time suggest a strong link of the EC with the way in which connectivity is achieved (Scheme 2). Thus, compound (III), which bridges metal centres through S—Ag junctions, presents the largest EC, surpassing the remaining t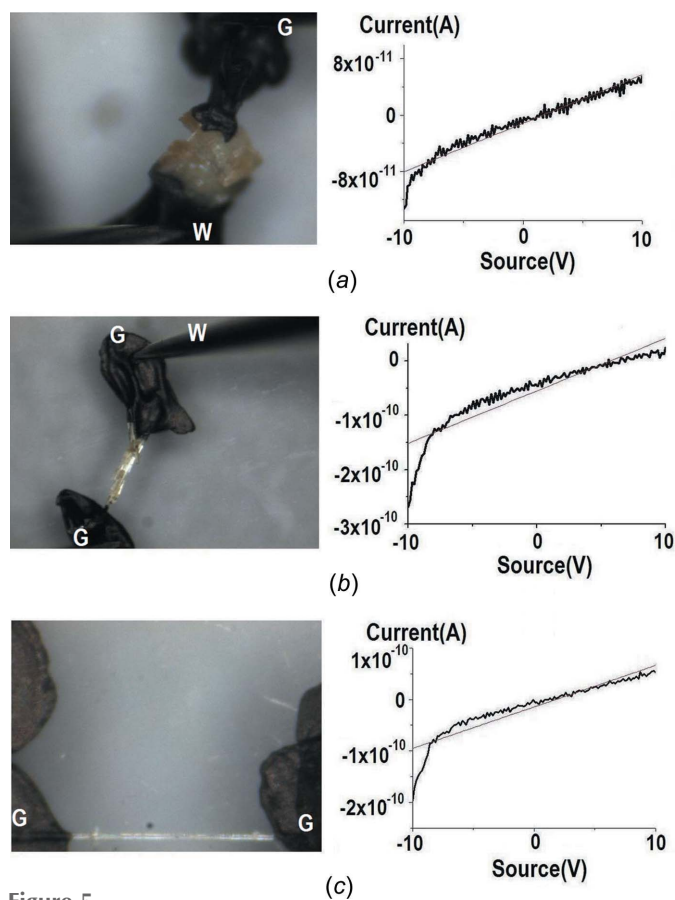wo by four orders of magnitude. On the other hand, in structures (I) and (II), where the bridges are formed *via* the N—Ag bonds of nitrogenated bases, the conductivity decreases dramatically. Analysis of these results seems to point to the Ag–S *versus* S–N connection mode of the bridging anion as a decisive factor, much more relevant than intermetallic interaction, and correlates with previously published data where the metal–sulfur connectivity seems to be the key in the electrical conductivity values *versus* metal–metal distances (Givaja *et al.*, 2012). It is clear that with such a poor casuistry, no conclusive assertion can be made on the subject and many more cases ought to be analyzed, but it certainly seems to be a topic worth considering in any further structural work on polymeric silver complexes.

References

Bader, R. F. W. (1990). In *Atoms in Molecules – a Quantum Theory*. Oxford University Press.
Becke, A. D. (1988). *Phys. Rev. A*, **38**, 3098–3100.
Becke, A. D. (1993). *J. Chem. Phys.* **98**, 5648–5652.
Bondi, A. (1964). *J. Phys. Chem.* **68**, 441–451.
Brown, I. D. (2002). In *The Chemical Bond in Inorganic Chemistry: The Bond Valence Model*. Oxford University Press.
Burrow, R. A., Belmonte, G. Z., Dorn, V. & Dennehy, M. (2016). *Inorg. Chim. Acta*, **450**, 39–49.
Cao, X. Y. & Dolg, M. (2002). *J. Mol. Struct. Theochem*, **581**, 139–147.
Castiñeiras, A., García-Santos, I., Dehnen, S. & Sevillano, P. (2006). *Polyhedron*, **25**, 3653–3660.
Dennehy, M., Delgado, F., Freire, E., Halac, E. & Baggio, R. (2016). *Acta Cryst.* C**72**, 572–577.
Dennehy, M., Ferullo, R. M., Quinzani, O. V., Mandolesi, S. D., Castellani, N. & Jennings, M. (2008). *Polyhedron*, **27**, 2243–2250.
Dennehy, M., Quinzani, O. V., Granados, A. & Burrow, R. A. (2010). *Polyhedron*, **29**, 1344–1352.
Dennehy, M., Quinzani, O. V. & Jennings, M. (2007). *J. Mol. Struct.* **841**, 110–117.
Ditchfield, R., Hehre, W. J. & Pople, J. A. (1971). *J. Chem. Phys.* **54**, 724–728.
Fuentealba, P., Preuss, H., Stoll, H. & Szentpaly, L. (1989). *Chem. Phys. Lett.* **89**, 418–422.
Givaja, G., Amo-Ochoa, P., Gómez-García, C. J. & Zamora, F. (2012). *Chem. Soc. Rev.* **41**, 115–147.
Groom, C. R., Bruno, I. J., Lightfoot, M. P. & Ward, S. C. (2016). *Acta Cryst.* B**72**, 171–179.
Harvey, P. D. (1996). *Coord. Chem. Rev.* **153**, 175–198.
Jansen, M. (1987). *Angew. Chem.* **99**, 1136–1149.
Kristiansson, O. (2001). *Inorg. Chem.* **40**, 5058–5059.
Lamming, G., Kolokotroni, J., Harrison, T., Penfold, T. J., Clegg, W., Waddell, P. G., Probert, M. R. & Houlton, A. (2017). *Cryst. Growth Des.* **17**, 5935–5944.
Lu, T. & Chen, F. (2012). *J. Comput. Chem.* **33**, 580–592.
Martina, I., Wiesinger, R., Jembrih-Simbürger, D. & Schreiner, M. (2012). *e-Preserv. Sci.* **9**, 1–8.
Morishima, Y., Young, D. J. & Fujisawa, K. (2014). *Dalton Trans.* **43**, 15915–15928.
Rassolov, V. A., Ratner, M. A., Pople, J. A., Redfern, P. C. & Curtiss, L. A. (2001). *J. Comput. Chem.* **22**, 976–984.
Rigaku OD (2015). *CrysAlis PRO*. Rigaku Oxford Diffraction, Yarnton, Oxfordshire, England.

Figure 5
(a) Left column: the set-up used for the measurement of electrical conductivity in monocrystals of (a) (I), (b) (II) and (c) (III). Right column: the corresponding EC curves. Lettering code: G is graphite paste and W is tungsten wires.

Schmidbaur, H. & Schier, A. (2015). *Angew. Chem. Int. Ed.* **54**, 746–784.

Schwerdtfeger, P., Dolg, M., Schwarz, W. H. E., Bowmaker, G. A. & Boyd, P. D. W. J. (1989). *Chem. Phys.* **91**, 1762–1774.

Serpe, A., Artizzu, F., Marchio, L., Mercuri, M. L., Pilia, L. & Deplano, P. (2001). *Cryst. Growth Des.* **2011**, 1278–1286.

Sheldrick, G. M. (2008). *Acta Cryst.* A**64**, 112–122.

Sheldrick, G. M. (2015). *Acta Cryst.* C**71**, 3–8.

Spek, A. L. (2009). *Acta Cryst.* D**65**, 148–155.

Su, W. P., Hong, M. C., Weng, J. B., Cao, R. & Lu, S. (2000). *Angew. Chem. Int. Ed.* **39**, 2911–2914.

Acta Cryst. (2018). C**74**, 186–193   Dennehy *et al.* · Argentophilic interactions in a silver thiosaccharinate complex   **193**

electronic reprint

Structure and electrical properties of a one-dimensional polymeric silver thiosaccharinate complex with argentophilic interactions

Mariana Dennehy, Pilar Amo-Ochoa, Eleonora Freire, Sebastián Suárez, Emilia Halac and Ricardo Baggio

Computing details

Data collection: *CrysAlis PRO* (Rigaku OD, 2015); cell refinement: *CrysAlis PRO* (Rigaku OD, 2015); data reduction: *CrysAlis PRO* (Rigaku OD, 2015); program(s) used to solve structure: *SHELXS97* (Sheldrick, 2008); program(s) used to refine structure: *SHELXL2014* (Sheldrick, 2015); molecular graphics: *XP* in *SHELXTL* (Sheldrick, 2008); software used to prepare material for publication: *SHELXL2014* (Sheldrick, 2015) and *PLATON* (Spek, 2009).

catena-Poly[[[aquatetrakis(μ_3-1,1-dioxo-1,2-benzisothiazole-3-thiolato-$\kappa^3 N$:S^3:S^3)tetrasilver(I)]-μ_2-4,4′-(propane-1,3-dyl)dipyridine-$\kappa^2 N$:N'] dimethyl sulfoxide hemisolvate]

Crystal data

[Ag$_4$(C$_7$H$_4$NO$_2$S$_2$)$_4$(C$_{13}$H$_{14}$N$_2$)(H$_2$O)]·0.5C$_2$H$_6$OS	$Z = 2$
$M_r = 1479.75$	$F(000) = 1458$
Triclinic, $P\bar{1}$	$D_x = 1.854$ Mg m^{-3}
$a = 13.7710$ (4) Å	Mo $K\alpha$ radiation, $\lambda = 0.71073$ Å
$b = 13.9822$ (4) Å	Cell parameters from 6300 reflections
$c = 14.7181$ (5) Å	$\theta = 3.6$–26.1°
$\alpha = 81.074$ (3)°	$\mu = 1.85$ mm^{-1}
$\beta = 79.523$ (3)°	$T = 290$ K
$\gamma = 73.152$ (3)°	Fragment, yellow
$V = 2651.23$ (15) Å^3	0.42 × 0.30 × 0.10 mm

Data collection

Rigaku OD Xcalibur Eos Gemini diffractometer	$T_{min} = 0.50$, $T_{max} = 0.85$
Radiation source: fine-focus sealed X-ray tube, Enhance (Mo) X-ray Source	26030 measured reflections
	11551 independent reflections
Graphite monochromator	7060 reflections with $I > 2\sigma(I)$
Detector resolution: 16.0604 pixels mm^{-1}	$R_{int} = 0.032$
ω scans	$\theta_{max} = 29.0°$, $\theta_{min} = 3.0°$
	$h = -17\rightarrow14$
Absorption correction: multi-scan (CrysAlis PRO; Rigaku OD, 2015)	$k = -19\rightarrow18$
	$l = -19\rightarrow19$

Refinement

Refinement on F^2	11551 reflections
Least-squares matrix: full	659 parameters
$R[F^2 > 2\sigma(F^2)] = 0.056$	62 restraints
$wR(F^2) = 0.158$	Hydrogen site location: mixed
$S = 1.03$	

H atoms treated by a mixture of independent and constrained refinement	$(\Delta/\sigma)_{max} = 0.001$

H atoms treated by a mixture of independent
   and constrained refinement
$w = 1/[\sigma^2(F_o^2) + (0.0606P)^2 + 6.6052P]$
   where $P = (F_o^2 + 2F_c^2)/3$

$(\Delta/\sigma)_{max} = 0.001$
$\Delta\rho_{max} = 1.17$ e Å^{-3}
$\Delta\rho_{min} = -0.85$ e Å^{-3}

Special details

Geometry. All esds (except the esd in the dihedral angle between two l.s. planes) are estimated using the full covariance matrix. The cell esds are taken into account individually in the estimation of esds in distances, angles and torsion angles; correlations between esds in cell parameters are only used when they are defined by crystal symmetry. An approximate (isotropic) treatment of cell esds is used for estimating esds involving l.s. planes.

Fractional atomic coordinates and isotropic or equivalent isotropic displacement parameters (Å²)

	x	y	z	$U_{iso}*/U_{eq}$	Occ. (<1)
Ag1	0.65543 (5)	0.22505 (5)	0.46035 (4)	0.07203 (19)	
Ag2	0.88094 (4)	0.27268 (4)	0.23224 (4)	0.06322 (17)	
Ag3	0.76014 (5)	0.09579 (5)	0.32270 (4)	0.06839 (18)	
Ag4	0.66209 (5)	0.30577 (4)	0.23040 (5)	0.07152 (19)	
S11	0.84966 (13)	0.21588 (13)	0.59344 (11)	0.0551 (4)	
S21	0.92920 (14)	0.10318 (14)	0.33902 (11)	0.0610 (5)	
O11	0.8151 (4)	0.1529 (4)	0.6700 (3)	0.0688 (13)	
O21	0.8090 (4)	0.3215 (4)	0.5947 (4)	0.0749 (14)	
N11	0.8288 (4)	0.1844 (4)	0.4955 (3)	0.0562 (14)	
C11	0.9170 (5)	0.1469 (5)	0.4442 (4)	0.0538 (16)	
C21	1.0095 (5)	0.1425 (5)	0.4830 (4)	0.0512 (15)	
C31	1.1124 (6)	0.1069 (6)	0.4467 (5)	0.069 (2)	
H31	1.131614	0.079417	0.390412	0.083*	
C41	1.1838 (6)	0.1136 (7)	0.4961 (6)	0.084 (3)	
H41	1.252856	0.091592	0.472183	0.100*	
C51	1.1575 (7)	0.1517 (7)	0.5798 (6)	0.086 (3)	
H51	1.208629	0.154018	0.612192	0.104*	
C61	1.0564 (6)	0.1865 (6)	0.6168 (5)	0.0663 (19)	
H61	1.038097	0.213381	0.673411	0.080*	
C71	0.9836 (5)	0.1804 (5)	0.5678 (4)	0.0508 (15)	
S12	0.90767 (14)	0.45315 (14)	0.35417 (13)	0.0613 (5)	
S22	0.62518 (13)	0.40188 (13)	0.36506 (14)	0.0599 (4)	
O12	0.9364 (4)	0.5197 (5)	0.2777 (4)	0.0888 (17)	
O22	0.9875 (4)	0.3742 (4)	0.3914 (4)	0.0771 (15)	
N12	0.8226 (4)	0.4027 (4)	0.3260 (4)	0.0542 (13)	
C12	0.7336 (5)	0.4323 (5)	0.3765 (4)	0.0547 (16)	
C22	0.7294 (5)	0.5008 (5)	0.4466 (5)	0.0561 (16)	
C32	0.6476 (6)	0.5427 (6)	0.5116 (6)	0.073 (2)	
H32	0.583357	0.532327	0.514579	0.087*	
C42	0.6658 (8)	0.6011 (7)	0.5723 (7)	0.099 (3)	
H42	0.613532	0.627817	0.618554	0.118*	
C52	0.7595 (9)	0.6196 (7)	0.5647 (8)	0.101 (3)	
H52	0.768754	0.660994	0.604262	0.121*	
C62	0.8403 (7)	0.5784 (6)	0.5000 (6)	0.081 (2)	
H62	0.904173	0.590096	0.495595	0.097*	

C72	0.8223 (6)	0.5191 (5)	0.4420 (5)	0.0603 (17)
S13	0.77183 (17)	−0.04495 (15)	0.14420 (12)	0.0661 (5)
S23	0.79677 (17)	0.24580 (16)	0.09670 (13)	0.0706 (5)
O13	0.6707 (5)	−0.0539 (5)	0.1495 (4)	0.0920 (18)
O23	0.8391 (6)	−0.1206 (5)	0.1963 (4)	0.099 (2)
N13	0.7665 (5)	0.0683 (4)	0.1702 (4)	0.0658 (16)
C13	0.8007 (6)	0.1233 (6)	0.0992 (4)	0.0605 (18)
C23	0.8414 (5)	0.0700 (6)	0.0148 (4)	0.0565 (17)
C33	0.8920 (6)	0.1030 (6)	−0.0706 (5)	0.072 (2)
H33	0.903369	0.166448	−0.082209	0.086*
C43	0.9246 (6)	0.0342 (7)	−0.1378 (5)	0.078 (2)
H43	0.958826	0.053267	−0.195180	0.094*
C53	0.9087 (6)	−0.0566 (7)	−0.1227 (6)	0.080 (2)
H53	0.929421	−0.097954	−0.170315	0.096*
C63	0.8618 (6)	−0.0909 (6)	−0.0375 (5)	0.0645 (18)
H63	0.852797	−0.155356	−0.026103	0.077*
C73	0.8295 (5)	−0.0260 (5)	0.0287 (4)	0.0566 (16)
S14	0.4768 (3)	0.2283 (3)	0.1562 (4)	0.1564 (19)
S24	0.58604 (17)	0.09204 (16)	0.40010 (14)	0.0744 (6)
O14	0.5430 (12)	0.2127 (11)	0.0714 (8)	0.224 (8)
O24	0.4002 (9)	0.3222 (7)	0.1609 (11)	0.239 (8)
N14	0.5432 (5)	0.2110 (5)	0.2431 (6)	0.093 (2)
C14	0.5281 (5)	0.1352 (5)	0.3060 (6)	0.070 (2)
C24	0.4566 (6)	0.0842 (6)	0.2798 (8)	0.084 (3)
C34	0.4227 (6)	0.0062 (7)	0.3280 (8)	0.098 (3)
H34	0.443561	−0.021910	0.385174	0.117*
C44	0.3593 (8)	−0.0302 (9)	0.2928 (12)	0.139 (5)
H44	0.334741	−0.082728	0.326089	0.167*
C54	0.3305 (11)	0.0102 (10)	0.2072 (14)	0.191 (9)
H54	0.290155	−0.018167	0.181236	0.230*
C64	0.3598 (11)	0.0901 (10)	0.1607 (14)	0.194 (9)
H64	0.338601	0.119274	0.103853	0.233*
C74	0.4222 (8)	0.1268 (8)	0.2002 (10)	0.116 (4)
N15	0.5352 (5)	0.2612 (5)	0.5904 (5)	0.0738 (18)
N25	0.0154 (5)	0.3171 (4)	1.1297 (4)	0.0636 (15)
C15	0.5497 (6)	0.3145 (6)	0.6487 (6)	0.081 (2)
H15	0.606869	0.339695	0.635095	0.097*
C25	0.4839 (7)	0.3354 (7)	0.7301 (7)	0.102 (3)
H25	0.497345	0.375572	0.768450	0.122*
C35	0.4003 (9)	0.2993 (8)	0.7563 (7)	0.117 (2)
C45	0.3833 (7)	0.2470 (7)	0.6937 (7)	0.099 (3)
H45	0.325658	0.222573	0.705694	0.118*
C55	0.4503 (6)	0.2293 (6)	0.6120 (6)	0.081 (2)
H55	0.435691	0.193616	0.570298	0.097*
C65	0.0985 (6)	0.3269 (7)	1.1586 (6)	0.084 (2)
H65	0.107427	0.305888	1.220409	0.101*
C75	0.1716 (6)	0.3668 (7)	1.1009 (8)	0.101 (3)
H75	0.227885	0.371349	1.124832	0.121*

C85	0.1632 (8)	0.3997 (7)	1.0092 (8)	0.108 (2)	
C95	0.0806 (6)	0.3843 (6)	0.9810 (6)	0.077 (2)	
H95	0.072422	0.400772	0.918608	0.092*	
C105	0.0090 (6)	0.3457 (5)	1.0403 (5)	0.0659 (19)	
H105	−0.046711	0.339131	1.016770	0.079*	
C115	0.3344 (8)	0.3133 (6)	0.8456 (7)	0.119 (2)	
H11A	0.281135	0.279603	0.849357	0.143*	
H11B	0.375009	0.280774	0.894774	0.143*	
C125	0.2860 (8)	0.4175 (6)	0.8625 (7)	0.117 (2)	
H12A	0.234327	0.443215	0.821442	0.140*	
H12B	0.337977	0.453345	0.840643	0.140*	
C135	0.2371 (8)	0.4496 (7)	0.9533 (6)	0.113 (2)	
H13A	0.202733	0.520722	0.944030	0.135*	
H13B	0.291114	0.442577	0.989975	0.135*	
S1A	0.6847 (8)	0.4079 (6)	0.8253 (6)	0.133 (3)	0.328 (5)
O1A	0.6320 (12)	0.4694 (10)	0.9058 (11)	0.186 (9)	0.328 (5)
C1A	0.8110 (12)	0.4169 (19)	0.7950 (17)	0.22 (2)	0.328 (5)
H1A	0.844439	0.378155	0.744136	0.330*	0.328 (5)
H1B	0.810526	0.485971	0.776836	0.330*	0.328 (5)
H1C	0.847147	0.391445	0.847388	0.330*	0.328 (5)
C2A	0.6862 (17)	0.2819 (7)	0.8598 (14)	0.127 (8)	0.328 (5)
H2A	0.719371	0.242681	0.809211	0.191*	0.328 (5)
H2B	0.722893	0.257230	0.911939	0.191*	0.328 (5)
H2C	0.617077	0.276749	0.877144	0.191*	0.328 (5)
S1B	0.7251 (11)	0.3810 (9)	0.8874 (12)	0.133 (3)	0.172 (5)
O1B	0.6320 (12)	0.4694 (10)	0.9058 (11)	0.186 (9)	0.172 (5)
C1B	0.8110 (12)	0.4169 (19)	0.7950 (17)	0.22 (2)	0.172 (5)
H1D	0.869773	0.360862	0.783539	0.330*	0.172 (5)
H1E	0.778031	0.438247	0.740327	0.330*	0.172 (5)
H1F	0.832267	0.471290	0.810252	0.330*	0.172 (5)
C2B	0.6862 (17)	0.2819 (7)	0.8598 (14)	0.127 (8)	0.172 (5)
H2D	0.744977	0.225914	0.848166	0.191*	0.172 (5)
H2E	0.639151	0.262109	0.910763	0.191*	0.172 (5)
H2F	0.653021	0.303303	0.805264	0.191*	0.172 (5)
O1W	0.5624 (10)	0.4406 (7)	0.1121 (8)	0.184 (5)	
H1WA	0.523 (13)	0.505 (4)	0.088 (12)	0.275*	
H1WB	0.550 (3)	0.395 (8)	0.077 (8)	0.275*	

Atomic displacement parameters (Å²)

	U^{11}	U^{22}	U^{33}	U^{12}	U^{13}	U^{23}
Ag1	0.0633 (4)	0.0866 (4)	0.0619 (4)	−0.0244 (3)	0.0095 (3)	−0.0088 (3)
Ag2	0.0624 (3)	0.0821 (4)	0.0466 (3)	−0.0265 (3)	0.0027 (2)	−0.0102 (3)
Ag3	0.0698 (4)	0.0936 (4)	0.0426 (3)	−0.0252 (3)	−0.0023 (3)	−0.0107 (3)
Ag4	0.0654 (4)	0.0731 (4)	0.0835 (4)	−0.0293 (3)	−0.0065 (3)	−0.0152 (3)
S11	0.0542 (10)	0.0723 (11)	0.0373 (8)	−0.0190 (8)	−0.0006 (7)	−0.0047 (7)
S21	0.0628 (11)	0.0771 (11)	0.0354 (8)	−0.0121 (9)	0.0025 (7)	−0.0081 (8)
O11	0.070 (3)	0.098 (4)	0.042 (3)	−0.038 (3)	−0.003 (2)	0.003 (2)

O21	0.072 (3)	0.074 (3)	0.071 (3)	−0.004 (3)	−0.004 (3)	−0.021 (3)
N11	0.051 (3)	0.074 (4)	0.037 (3)	−0.007 (3)	−0.007 (2)	−0.005 (2)
C11	0.049 (4)	0.069 (4)	0.039 (3)	−0.016 (3)	−0.006 (3)	0.006 (3)
C21	0.054 (4)	0.052 (3)	0.042 (3)	−0.015 (3)	−0.002 (3)	0.006 (3)
C31	0.052 (4)	0.095 (5)	0.052 (4)	−0.013 (4)	0.001 (3)	−0.004 (4)
C41	0.053 (5)	0.128 (7)	0.063 (5)	−0.024 (5)	−0.009 (4)	0.009 (5)
C51	0.061 (5)	0.123 (7)	0.079 (6)	−0.035 (5)	−0.024 (5)	0.012 (5)
C61	0.073 (5)	0.077 (5)	0.052 (4)	−0.028 (4)	−0.018 (4)	0.009 (3)
C71	0.050 (4)	0.060 (4)	0.043 (3)	−0.020 (3)	−0.009 (3)	0.007 (3)
S12	0.0549 (10)	0.0743 (11)	0.0622 (11)	−0.0306 (9)	−0.0107 (8)	−0.0019 (9)
S22	0.0451 (9)	0.0628 (10)	0.0737 (12)	−0.0176 (8)	−0.0049 (8)	−0.0112 (9)
O12	0.079 (4)	0.109 (4)	0.090 (4)	−0.059 (3)	−0.010 (3)	0.012 (3)
O22	0.057 (3)	0.088 (4)	0.087 (4)	−0.015 (3)	−0.016 (3)	−0.013 (3)
N12	0.047 (3)	0.060 (3)	0.058 (3)	−0.020 (3)	−0.001 (3)	−0.012 (3)
C12	0.062 (4)	0.060 (4)	0.047 (4)	−0.027 (3)	−0.009 (3)	0.002 (3)
C22	0.055 (4)	0.052 (4)	0.060 (4)	−0.010 (3)	−0.014 (3)	−0.004 (3)
C32	0.054 (4)	0.079 (5)	0.083 (5)	−0.004 (4)	−0.014 (4)	−0.024 (4)
C42	0.095 (7)	0.094 (6)	0.104 (7)	−0.003 (6)	−0.017 (6)	−0.042 (6)
C52	0.105 (8)	0.083 (6)	0.127 (9)	−0.011 (6)	−0.034 (7)	−0.053 (6)
C62	0.091 (6)	0.074 (5)	0.092 (6)	−0.028 (5)	−0.031 (5)	−0.015 (5)
C72	0.064 (5)	0.058 (4)	0.063 (4)	−0.018 (3)	−0.022 (4)	−0.003 (3)
S13	0.0841 (14)	0.0762 (12)	0.0419 (9)	−0.0343 (11)	−0.0004 (9)	−0.0039 (8)
S23	0.0935 (15)	0.0871 (13)	0.0480 (10)	−0.0530 (12)	−0.0116 (10)	−0.0007 (9)
O13	0.088 (4)	0.102 (4)	0.093 (4)	−0.051 (3)	0.019 (3)	−0.018 (3)
O23	0.138 (6)	0.094 (4)	0.060 (3)	−0.027 (4)	−0.029 (4)	0.015 (3)
N13	0.090 (5)	0.080 (4)	0.035 (3)	−0.042 (3)	0.003 (3)	−0.007 (3)
C13	0.072 (5)	0.091 (5)	0.034 (3)	−0.045 (4)	−0.009 (3)	−0.006 (3)
C23	0.050 (4)	0.094 (5)	0.031 (3)	−0.027 (4)	−0.009 (3)	−0.002 (3)
C33	0.070 (5)	0.099 (6)	0.049 (4)	−0.040 (4)	−0.001 (4)	0.006 (4)
C43	0.076 (5)	0.120 (7)	0.032 (4)	−0.027 (5)	0.007 (3)	−0.005 (4)
C53	0.076 (6)	0.104 (7)	0.055 (5)	−0.019 (5)	0.000 (4)	−0.015 (4)
C63	0.066 (5)	0.075 (5)	0.049 (4)	−0.009 (4)	−0.009 (3)	−0.013 (3)
C73	0.056 (4)	0.072 (4)	0.042 (4)	−0.019 (3)	−0.010 (3)	0.000 (3)
S14	0.156 (3)	0.136 (3)	0.223 (4)	−0.100 (3)	−0.140 (3)	0.094 (3)
S24	0.0768 (13)	0.0880 (13)	0.0605 (11)	−0.0384 (11)	0.0086 (10)	−0.0054 (10)
O14	0.323 (17)	0.298 (15)	0.148 (9)	−0.224 (14)	−0.170 (11)	0.113 (10)
O24	0.176 (10)	0.115 (6)	0.46 (2)	−0.062 (7)	−0.210 (13)	0.117 (9)
N14	0.080 (5)	0.084 (4)	0.128 (6)	−0.045 (4)	−0.052 (5)	0.035 (4)
C14	0.049 (4)	0.053 (4)	0.103 (6)	−0.015 (3)	0.004 (4)	−0.011 (4)
C24	0.049 (4)	0.063 (5)	0.139 (8)	−0.020 (4)	−0.011 (5)	−0.004 (5)
C34	0.054 (5)	0.082 (6)	0.162 (10)	−0.037 (4)	−0.003 (5)	−0.003 (6)
C44	0.082 (7)	0.101 (8)	0.245 (17)	−0.049 (6)	−0.049 (9)	0.024 (9)
C54	0.162 (13)	0.130 (10)	0.34 (2)	−0.101 (10)	−0.171 (16)	0.085 (13)
C64	0.173 (13)	0.129 (10)	0.34 (2)	−0.090 (10)	−0.191 (15)	0.083 (12)
C74	0.087 (7)	0.102 (7)	0.180 (11)	−0.051 (6)	−0.069 (8)	0.033 (7)
N15	0.054 (4)	0.089 (4)	0.072 (4)	−0.022 (3)	0.015 (3)	−0.012 (4)
N25	0.058 (4)	0.079 (4)	0.053 (3)	−0.024 (3)	0.006 (3)	−0.010 (3)
C15	0.059 (5)	0.083 (5)	0.093 (6)	−0.017 (4)	0.014 (4)	−0.020 (5)

C25	0.095 (7)	0.094 (6)	0.112 (8)	−0.035 (5)	0.040 (6)	−0.048 (6)
C35	0.114 (4)	0.100 (4)	0.124 (4)	−0.051 (3)	0.066 (4)	−0.033 (3)
C45	0.076 (6)	0.093 (6)	0.113 (8)	−0.033 (5)	0.036 (5)	−0.009 (6)
C55	0.069 (5)	0.093 (6)	0.072 (5)	−0.019 (5)	0.005 (4)	−0.006 (4)
C65	0.063 (5)	0.125 (7)	0.068 (5)	−0.030 (5)	−0.006 (4)	−0.018 (5)
C75	0.037 (4)	0.118 (7)	0.148 (10)	−0.031 (5)	0.022 (5)	−0.037 (7)
C85	0.103 (4)	0.096 (4)	0.120 (4)	−0.053 (3)	0.062 (4)	−0.039 (3)
C95	0.074 (5)	0.077 (5)	0.067 (5)	−0.023 (4)	0.025 (4)	−0.007 (4)
C105	0.057 (4)	0.071 (4)	0.068 (5)	−0.020 (4)	0.005 (4)	−0.011 (4)
C115	0.116 (4)	0.103 (3)	0.126 (4)	−0.051 (3)	0.066 (3)	−0.032 (3)
C125	0.113 (4)	0.102 (3)	0.125 (4)	−0.052 (3)	0.064 (3)	−0.033 (3)
C135	0.107 (4)	0.100 (3)	0.123 (4)	−0.053 (3)	0.062 (3)	−0.036 (3)
S1A	0.193 (10)	0.098 (5)	0.105 (7)	−0.011 (6)	−0.056 (6)	−0.015 (5)
O1A	0.19 (2)	0.145 (15)	0.19 (2)	0.001 (14)	0.008 (16)	−0.073 (14)
C1A	0.20 (3)	0.22 (3)	0.30 (4)	−0.13 (3)	0.07 (3)	−0.21 (3)
C2A	0.14 (2)	0.123 (17)	0.103 (16)	0.016 (15)	−0.065 (15)	−0.003 (13)
S1B	0.193 (10)	0.098 (5)	0.105 (7)	−0.011 (6)	−0.056 (6)	−0.015 (5)
O1B	0.19 (2)	0.145 (15)	0.19 (2)	0.001 (14)	0.008 (16)	−0.073 (14)
C1B	0.20 (3)	0.22 (3)	0.30 (4)	−0.13 (3)	0.07 (3)	−0.21 (3)
C2B	0.14 (2)	0.123 (17)	0.103 (16)	0.016 (15)	−0.065 (15)	−0.003 (13)
O1W	0.231 (12)	0.141 (7)	0.220 (11)	−0.094 (8)	−0.116 (9)	0.041 (7)

Geometric parameters (Å, º)

Ag1—N15	2.307 (6)	C63—H63	0.9300
Ag1—N11	2.422 (5)	S14—O14	1.411 (15)
Ag1—S22	2.607 (2)	S14—O24	1.429 (12)
Ag1—S24	2.647 (2)	S14—N14	1.653 (8)
Ag1—Ag3	2.8307 (8)	S14—C74	1.776 (10)
Ag2—N12	2.320 (5)	S24—C14	1.668 (9)
Ag2—N25i	2.335 (6)	N14—C14	1.333 (10)
Ag2—S23	2.606 (2)	C14—C24	1.502 (11)
Ag2—S21	2.615 (2)	C24—C74	1.331 (14)
Ag2—Ag4	2.9180 (8)	C24—C34	1.359 (11)
Ag2—Ag3	3.3489 (8)	C34—C44	1.340 (14)
Ag3—N13	2.317 (5)	C34—H34	0.9300
Ag3—S21	2.416 (2)	C44—C54	1.376 (19)
Ag3—S24	2.472 (2)	C44—H44	0.9300
Ag3—Ag4	3.0692 (9)	C54—C64	1.343 (17)
Ag4—N14	2.354 (6)	C54—H54	0.9300
Ag4—S22	2.461 (2)	C64—C74	1.367 (15)
Ag4—S23	2.510 (2)	C64—H64	0.9300
Ag4—O1W	2.612 (9)	N15—C15	1.296 (10)
S11—O11	1.418 (5)	N15—C55	1.337 (10)
S11—O21	1.421 (5)	N25—C105	1.325 (9)
S11—N11	1.665 (6)	N25—C65	1.340 (10)
S11—C71	1.751 (7)	C15—C25	1.379 (11)
S21—C11	1.714 (7)	C15—H15	0.9300

N11—C11	1.319 (8)	C25—C35	1.358 (13)
C11—C21	1.470 (9)	C25—H25	0.9300
C21—C71	1.379 (9)	C35—C45	1.351 (14)
C21—C31	1.393 (9)	C35—C115	1.460 (6)
C31—C41	1.355 (11)	C45—C55	1.384 (11)
C31—H31	0.9300	C45—H45	0.9300
C41—C51	1.364 (12)	C55—H55	0.9300
C41—H41	0.9300	C65—C75	1.384 (12)
C51—C61	1.373 (11)	C65—H65	0.9300
C51—H51	0.9300	C75—C85	1.370 (15)
C61—C71	1.365 (9)	C75—H75	0.9300
C61—H61	0.9300	C85—C95	1.362 (14)
S12—O12	1.420 (6)	C85—C135	1.460 (6)
S12—O22	1.434 (5)	C95—C105	1.369 (10)
S12—N12	1.670 (6)	C95—H95	0.9300
S12—C72	1.759 (8)	C105—H105	0.9300
S22—C12	1.709 (7)	C115—C125	1.455 (6)
N12—C12	1.302 (8)	C115—H11A	0.9700
C12—C22	1.496 (9)	C115—H11B	0.9700
C22—C72	1.363 (10)	C125—C135	1.457 (6)
C22—C32	1.387 (10)	C125—H12A	0.9700
C32—C42	1.399 (12)	C125—H12B	0.9700
C32—H32	0.9300	C135—H13A	0.9700
C42—C52	1.370 (13)	C135—H13B	0.9700
C42—H42	0.9300	S1A—O1A	1.520 (3)
C52—C62	1.374 (13)	S1A—C1A	1.751 (3)
C52—H52	0.9300	S1A—C2A	1.752 (3)
C62—C72	1.376 (10)	C1A—H1A	0.9600
C62—H62	0.9300	C1A—H1B	0.9600
S13—O23	1.415 (6)	C1A—H1C	0.9600
S13—O13	1.421 (6)	C2A—H2A	0.9600
S13—N13	1.664 (6)	C2A—H2B	0.9600
S13—C73	1.756 (7)	C2A—H2C	0.9600
S23—C13	1.693 (8)	S1B—O1B	1.517 (3)
N13—C13	1.300 (8)	S1B—C1B	1.746 (3)
C13—C23	1.485 (9)	S1B—C2B	1.749 (3)
C23—C73	1.379 (10)	C1B—H1D	0.9600
C23—C33	1.403 (9)	C1B—H1E	0.9600
C33—C43	1.409 (11)	C1B—H1F	0.9600
C33—H33	0.9300	C2B—H2D	0.9600
C43—C53	1.330 (11)	C2B—H2E	0.9600
C43—H43	0.9300	C2B—H2F	0.9600
C53—C63	1.384 (10)	O1W—H1WA	0.956 (10)
C53—H53	0.9300	O1W—H1WB	0.953 (10)
C63—C73	1.362 (9)		
N15—Ag1—N11	111.9 (2)	C73—C23—C13	112.0 (6)
N15—Ag1—S22	100.45 (17)	C33—C23—C13	128.7 (7)

N11—Ag1—S22	105.35 (14)	C23—C33—C43	116.0 (7)
N15—Ag1—S24	99.32 (19)	C23—C33—H33	122.0
N11—Ag1—S24	121.61 (14)	C43—C33—H33	122.0
S22—Ag1—S24	116.15 (7)	C53—C43—C33	122.9 (7)
N15—Ag1—Ag3	150.49 (18)	C53—C43—H43	118.6
N11—Ag1—Ag3	79.72 (13)	C33—C43—H43	118.6
S22—Ag1—Ag3	102.32 (5)	C43—C53—C63	121.4 (8)
S24—Ag1—Ag3	53.52 (5)	C43—C53—H53	119.3
N12—Ag2—N25i	102.99 (19)	C63—C53—H53	119.3
N12—Ag2—S23	127.40 (15)	C73—C63—C53	116.9 (8)
N25i—Ag2—S23	92.24 (16)	C73—C63—H63	121.6
N12—Ag2—S21	108.22 (14)	C53—C63—H63	121.6
N25i—Ag2—S21	116.38 (16)	C63—C73—C23	123.5 (6)
S23—Ag2—S21	109.02 (6)	C63—C73—S13	129.4 (6)
N12—Ag2—Ag4	82.64 (13)	C23—C73—S13	107.1 (5)
N25i—Ag2—Ag4	135.26 (16)	O14—S14—O24	117.3 (8)
S23—Ag2—Ag4	53.68 (5)	O14—S14—N14	110.7 (6)
S21—Ag2—Ag4	103.06 (5)	O24—S14—N14	108.5 (7)
N12—Ag2—Ag3	107.90 (13)	O14—S14—C74	113.0 (8)
N25i—Ag2—Ag3	148.13 (15)	O24—S14—C74	110.7 (7)
S23—Ag2—Ag3	75.23 (4)	N14—S14—C74	94.2 (5)
S21—Ag2—Ag3	45.78 (5)	C14—S24—Ag3	96.3 (3)
Ag4—Ag2—Ag3	58.163 (19)	C14—S24—Ag1	114.3 (3)
N13—Ag3—S21	106.92 (16)	Ag3—S24—Ag1	67.04 (6)
N13—Ag3—S24	105.52 (17)	C14—N14—S14	112.5 (6)
S21—Ag3—S24	147.31 (7)	C14—N14—Ag4	129.5 (6)
N13—Ag3—Ag1	143.77 (16)	S14—N14—Ag4	117.5 (4)
S21—Ag3—Ag1	95.14 (5)	N14—C14—C24	112.3 (8)
S24—Ag3—Ag1	59.44 (5)	N14—C14—S24	126.2 (6)
N13—Ag3—Ag4	76.88 (15)	C24—C14—S24	121.4 (6)
S21—Ag3—Ag4	103.82 (5)	C74—C24—C34	119.4 (9)
S24—Ag3—Ag4	87.29 (6)	C74—C24—C14	112.3 (8)
Ag1—Ag3—Ag4	70.03 (2)	C34—C24—C14	128.2 (10)
N13—Ag3—Ag2	85.74 (14)	C44—C34—C24	119.7 (12)
S21—Ag3—Ag2	50.87 (5)	C44—C34—H34	120.1
S24—Ag3—Ag2	136.51 (6)	C24—C34—H34	120.1
Ag1—Ag3—Ag2	86.51 (2)	C34—C44—C54	119.8 (11)
Ag4—Ag3—Ag2	53.872 (18)	C34—C44—H44	120.1
N14—Ag4—S22	110.2 (2)	C54—C44—H44	120.1
N14—Ag4—S23	105.5 (2)	C64—C54—C44	121.0 (12)
S22—Ag4—S23	143.14 (7)	C64—C54—H54	119.5
N14—Ag4—O1W	90.5 (3)	C44—C54—H54	119.5
S22—Ag4—O1W	100.3 (3)	C54—C64—C74	117.2 (13)
S23—Ag4—O1W	88.2 (3)	C54—C64—H64	121.4
N14—Ag4—Ag2	138.93 (18)	C74—C64—H64	121.4
S22—Ag4—Ag2	89.29 (5)	C24—C74—C64	122.5 (10)
S23—Ag4—Ag2	56.79 (5)	C24—C74—S14	108.7 (7)
O1W—Ag4—Ag2	122.1 (3)	C64—C74—S14	128.6 (10)

N14—Ag4—Ag3	73.22 (16)	C15—N15—C55	116.2 (7)
S22—Ag4—Ag3	99.45 (5)	C15—N15—Ag1	119.2 (5)
S23—Ag4—Ag3	81.93 (5)	C55—N15—Ag1	124.6 (6)
O1W—Ag4—Ag3	157.8 (2)	C105—N25—C65	115.3 (7)
Ag2—Ag4—Ag3	67.97 (2)	C105—N25—Ag2ii	121.8 (5)
O11—S11—O21	117.6 (3)	C65—N25—Ag2ii	122.4 (5)
O11—S11—N11	109.3 (3)	N15—C15—C25	122.7 (8)
O21—S11—N11	108.5 (3)	N15—C15—H15	118.7
O11—S11—C71	111.1 (3)	C25—C15—H15	118.7
O21—S11—C71	112.3 (3)	C35—C25—C15	122.4 (9)
N11—S11—C71	95.7 (3)	C35—C25—H25	118.8
C11—S21—Ag3	106.1 (2)	C15—C25—H25	118.8
C11—S21—Ag2	100.6 (2)	C45—C35—C25	114.7 (8)
Ag3—S21—Ag2	83.35 (6)	C45—C35—C115	121.9 (10)
C11—N11—S11	110.0 (5)	C25—C35—C115	123.4 (10)
C11—N11—Ag1	130.0 (4)	C35—C45—C55	121.0 (9)
S11—N11—Ag1	119.7 (3)	C35—C45—H45	119.5
N11—C11—C21	115.8 (6)	C55—C45—H45	119.5
N11—C11—S21	124.7 (5)	N15—C55—C45	123.0 (9)
C21—C11—S21	119.5 (5)	N15—C55—H55	118.5
C71—C21—C31	119.6 (7)	C45—C55—H55	118.5
C71—C21—C11	110.7 (6)	N25—C65—C75	123.0 (9)
C31—C21—C11	129.7 (6)	N25—C65—H65	118.5
C41—C31—C21	117.9 (7)	C75—C65—H65	118.5
C41—C31—H31	121.0	C85—C75—C65	121.7 (9)
C21—C31—H31	121.0	C85—C75—H75	119.2
C31—C41—C51	122.0 (8)	C65—C75—H75	119.2
C31—C41—H41	119.0	C75—C85—C95	113.8 (7)
C51—C41—H41	119.0	C75—C85—C135	119.6 (12)
C41—C51—C61	120.8 (8)	C95—C85—C135	126.6 (12)
C41—C51—H51	119.6	C105—C95—C85	122.9 (9)
C61—C51—H51	119.6	C105—C95—H95	118.6
C71—C61—C51	117.9 (8)	C85—C95—H95	118.6
C71—C61—H61	121.1	N25—C105—C95	123.1 (8)
C51—C61—H61	121.1	N25—C105—H105	118.4
C61—C71—C21	121.7 (6)	C95—C105—H105	118.4
C61—C71—S11	130.4 (6)	C125—C115—C35	115.0 (8)
C21—C71—S11	107.9 (5)	C125—C115—H11A	108.5
O12—S12—O22	117.9 (4)	C35—C115—H11A	108.5
O12—S12—N12	109.1 (3)	C125—C115—H11B	108.5
O22—S12—N12	108.9 (3)	C35—C115—H11B	108.5
O12—S12—C72	111.5 (4)	H11A—C115—H11B	107.5
O22—S12—C72	111.7 (3)	C115—C125—C135	124.1 (9)
N12—S12—C72	95.3 (3)	C115—C125—H12A	106.3
C12—S22—Ag4	108.8 (2)	C135—C125—H12A	106.3
C12—S22—Ag1	100.2 (2)	C115—C125—H12B	106.3
Ag4—S22—Ag1	83.95 (6)	C135—C125—H12B	106.3
C12—N12—S12	110.8 (5)	H12A—C125—H12B	106.4

C12—N12—Ag2	129.0 (4)	C125—C135—C85	119.3 (8)
S12—N12—Ag2	118.8 (3)	C125—C135—H13A	107.5
N12—C12—C22	115.1 (6)	C85—C135—H13A	107.5
N12—C12—S22	125.0 (5)	C125—C135—H13B	107.5
C22—C12—S22	119.9 (5)	C85—C135—H13B	107.5
C72—C22—C32	120.3 (7)	H13A—C135—H13B	107.0
C72—C22—C12	110.8 (6)	O1A—S1A—C1A	109.3 (6)
C32—C22—C12	128.9 (7)	O1A—S1A—C2A	109.1 (6)
C22—C32—C42	117.3 (8)	C1A—S1A—C2A	109.2 (12)
C22—C32—H32	121.3	S1A—C1A—H1A	109.5
C42—C32—H32	121.3	S1A—C1A—H1B	109.5
C52—C42—C32	120.9 (9)	H1A—C1A—H1B	109.5
C52—C42—H42	119.6	S1A—C1A—H1C	109.5
C32—C42—H42	119.6	H1A—C1A—H1C	109.5
C42—C52—C62	121.6 (8)	H1B—C1A—H1C	109.5
C42—C52—H52	119.2	S1A—C2A—H2A	109.5
C62—C52—H52	119.2	S1A—C2A—H2B	109.5
C72—C62—C52	117.0 (8)	H2A—C2A—H2B	109.5
C72—C62—H62	121.5	S1A—C2A—H2C	109.5
C52—C62—H62	121.5	H2A—C2A—H2C	109.5
C22—C72—C62	122.9 (7)	H2B—C2A—H2C	109.5
C22—C72—S12	108.1 (5)	O1B—S1B—C1B	109.6 (6)
C62—C72—S12	129.1 (6)	O1B—S1B—C2B	109.3 (7)
O23—S13—O13	117.0 (4)	C1B—S1B—C2B	109.6 (12)
O23—S13—N13	110.4 (4)	S1B—C1B—H1D	109.5
O13—S13—N13	109.4 (4)	S1B—C1B—H1E	109.5
O23—S13—C73	110.9 (4)	H1D—C1B—H1E	109.5
O13—S13—C73	111.9 (4)	S1B—C1B—H1F	109.5
N13—S13—C73	95.0 (3)	H1D—C1B—H1F	109.5
C13—S23—Ag4	104.2 (2)	H1E—C1B—H1F	109.5
C13—S23—Ag2	110.9 (2)	S1B—C2B—H2D	109.5
Ag4—S23—Ag2	69.53 (5)	S1B—C2B—H2E	109.5
C13—N13—S13	112.2 (5)	H2D—C2B—H2E	109.5
C13—N13—Ag3	123.1 (5)	S1B—C2B—H2F	109.5
S13—N13—Ag3	120.6 (3)	H2D—C2B—H2F	109.5
N13—C13—C23	113.6 (6)	H2E—C2B—H2F	109.5
N13—C13—S23	125.5 (5)	Ag4—O1W—H1WA	158 (9)
C23—C13—S23	120.9 (5)	Ag4—O1W—H1WB	97 (9)
C73—C23—C33	119.2 (7)	H1WA—O1W—H1WB	103.4 (15)

Symmetry codes: (i) $x+1$, y, $z-1$; (ii) $x-1$, y, $z+1$.

Hydrogen-bond geometry (Å, º)

D—H···A	D—H	H···A	D···A	D—H···A
O1W—H1WB···O14	0.95 (10)	2.59 (11)	3.425 (18)	147 (9)
O1W—H1WB···O24	0.95 (10)	2.59 (8)	3.072 (18)	112 (8)
O1W—H1WA···O1A[iii]	0.96 (9)	2.05 (18)	2.65 (2)	119 (12)

C125—H12B···O1W[iii]	0.97	2.53	3.369 (17)	144
C44—H44···O11[iv]	0.93	2.52	3.260 (13)	137
C53—H53···S21[v]	0.93	2.86	3.572 (9)	134
C75—H75···O24[vi]	0.93	2.41	3.284 (16)	158
C105—H105···S23[ii]	0.93	2.82	3.508 (9)	132

Symmetry codes: (ii) $x-1$, y, $z+1$; (iii) $-x+1$, $-y+1$, $-z+1$; (iv) $-x+1$, $-y$, $-z+1$; (v) $-x+2$, $-y$, $-z$; (vi) x, y, $z+1$.